Scattering matrix method for modeling acoustic waves in piezoelectric, fluid, and metallic multilayers

Alexandre Reinhardt,[a] Thomas Pastureaud, Sylvain Ballandras, and Vincent Laude
Laboratoire de Physique et Métrologie des Oscillateurs, CNRS UPR 3203, associé à l'Université de Franche-Comté, 32 avenue de l'Observatoire, 25044 Besançon cedex, France

(Received 6 January 2003; accepted 2 September 2003)

Many ultrasonic devices, among which are surface and bulk acoustic wave devices and ultrasonic transducers, are based on multilayers of heterogeneous materials, i.e., piezoelectrics, dielectrics, metals, and conducting or insulating fluids. We introduce metal and fluid layers and half spaces into a numerically stable scattering matrix model originally proposed for solving the problem of plane wave propagation in piezoelectric and dielectric multilayers. The method is stable for arbitrary thicknesses of the layers. We discuss how the surface Green's functions can be computed for an arbitrary stack of homogeneous materials with plane interfaces. Aditionnally, we set up a backscattering algorithm to compute the distribution of electromechanical fields at any point in the stack. The model is assessed by considering some well-known examples. © *2003 American Institute of Physics.* [DOI: 10.1063/1.1621053]

I. INTRODUCTION

There are many situations in ultrasonics in which one is dealing with multilayers of heterogeneous materials. For instance, surface acoustic wave and bulk acoustic wave devices, such as film bulk acoustic resonators, rely on the excitation of a piezoelectric substrate or of a piezoelectric stack by metallic electrodes. They can operate in air, which can be modeled as an insulating fluid, or in some special cases in water, which is usually considered a conducting fluid. Ultrasonic transducers also require a combination of piezoelectric, insulating, and metallic materials, and often operate in fluids. In the very common case that the interfaces are plane and the materials are homogeneous inside each layer, it is practical and efficient to solve the problem of plane wave propagation in the multilayer. Specifically, from this spectral domain approach the Green's function, surface effective permittivity, or admittance can be obtained. The purpose of this work is to present a numerically stable scattering matrix method solving the plane wave propagation problem in heterogeneous multilayers of piezoelectric, fluid, and metallic materials.

Fahmy and Adler have proposed a model based on a transfer matrix approach[1,2] to solve the plane wave propagation problem in piezoelectric multilayers, including dielectrics as a subcase. The plane wave solution of the propagation problem is described as the superposition of eight partial waves in each layer. The global plane wave solutions in a stack of materials are obtained by transferring boundary conditions from one interface to the other and then solving a linear system. The advantage over previous methods, such as the global matrix method (see, e.g., Ref. 3, for a review), is that the global linear system remains of constant size for any number of layers. Although very powerful, this approach suffers from numerical instabilities when the thicknesses of the layers or the frequency become too high.[4,5] When expressing electromechanical fields at an interface as a function of fields at the opposite interface of the same layer, one needs to calculate exponentials which for inhomogeneous partial waves can become either very large or very small. When mixing these terms, numerical underflows can occur while the decreasing terms get lost. Recently, independently and nearly simultaneously, Pastureaud *et al.*[4] and Tan[5] have proposed a stable solution based on the use of scattering matrices instead of transfer matrices. However, all these methods currently apply only to piezoelectric or dielectric layers.

In this article, we extend the scattering matrix method to metals, so that the finite width of electrodes included in multilayer structures can be taken into account, and also fluids, either insulating like air, or conducting like water. In Sec. II, after a short review of the so-called Fahmy–Adler formalism for piezoelectric and dielectric layers, we discuss how metal and fluid layers can also be described by a similar formalism. In Sec. III, we give an overview of the general scattering matrix algorithm presented in Ref. 4, and we extend it to metal and fluid materials. In Sec. IV, the computation of Green's functions is outlined and illustrated with the example of a structure involving piezoelectric, metal, and fluid layers. In Sec. V, it is shown how physical quantities of interest, such as displacements, stresses, electric potential, and displacement, can be determined in the whole stack of materials by a simple backscattering algorithm. An example is given to illustrate the interest of these calculations.

II. PLANE WAVE PROPAGATION

We consider the general case of a multilayer structure of infinite extent in the x_1 and x_3 directions, assuming axes conventions given in Fig. 1. We refer to each layer through its index n ranging from 1 for the bottom-most layer to N for the topmost layer. Each layer is assumed to be homogeneous and of constant thickness t_n.

We first focus on the problem of finding the characteristics of monochromatic plane waves propagating in a layer. Assuming a propagation along the horizontal plane with

[a]Electronic mail: alexandre.reinhardt@lpmo.edu

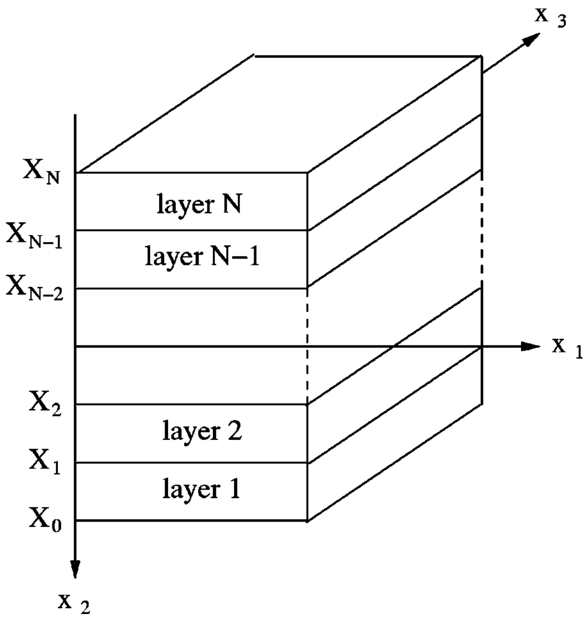

FIG. 1. Definition of a multilayered structure.

slownesses s_1 and s_3, all physical quantities have a dependency of the form $\exp[j\omega(t-s_1x_1-s_2x_2-s_3x_3)]$.

A. Fahmy–Adler solution

Fahmy and Adler[2] have proposed an elegant way of solving the propagation problem in a homogeneous piezoelectric layer. They start from the equations of piezoelectricity:[6]

$$T_{ij}=c_{ijkl}S_{kl}-e_{lij}E_l, \tag{1}$$

$$D_i=e_{ikl}S_{kl}+\epsilon_{ij}E_j, \tag{2}$$

where c_{ijkl}, e_{lij}, and ϵ_{ij} are, respectively, the components of the elastic, piezoelectric, and dielectric tensors, while T_{ij} and S_{kl} are the components of the stress and strain tensors, and D_i and E_j are the components of the electric displacement and field, respectively. The strain and electric field can be related to the mechanical displacements u_i and the electric potential ϕ by the relations

$$S_{kl}=\frac{1}{2}\left(\frac{\partial u_k}{\partial x_l}+\frac{\partial u_l}{\partial x_k}\right), \tag{3}$$

$$E_l=-\frac{\partial \phi}{\partial x_l}. \tag{4}$$

Equation (4) is a consequence of the quasistatic approximation. Assuming harmonic time and space dependences, Eqs. (1)–(4) become

$$T_{ij}=-j\omega s_l(c_{ijkl}u_k+e_{lij}\phi), \tag{5}$$

$$D_i=-j\omega s_l(e_iklu_k-\epsilon_{il}\phi). \tag{6}$$

For convenience of notation, we introduce vectors of generalized displacements and stresses:

$$\mathbf{u}=(u_1\ \ u_2\ \ u_3\ \ \phi)^T, \tag{7}$$

$$\tau_i=(\tau_{i1}\ \ \tau_{i2}\ \ \tau_{i3}\ \ \mathcal{D}_i)^T, \tag{8}$$

with $\tau_{ij}=-T_{ij}/j\omega$ and $\mathcal{D}_i=D_i/j\omega$. These vectors allow us to rewrite Eqs. (5) and (6) using matrix relations

$$\tau_i=(s_1A_{i1}+s_2A_{i2}+s_3A_{i3})\mathbf{u}, \tag{9}$$

where the A_{il} matrices are functions of the material constants:

$$A_{il}=\begin{pmatrix} c_{i11l} & c_{i12l} & c_{i13l} & e_{li1} \\ c_{i21l} & c_{i22l} & c_{i23l} & e_{li2} \\ c_{i31l} & c_{i32l} & c_{i33l} & e_{li3} \\ e_{i1l} & e_{i2l} & e_{i3l} & -\epsilon_{il} \end{pmatrix}. \tag{10}$$

Using the symmetry relations of material tensors, it is possible to show that

$$A_{il}=A_{li}^T. \tag{11}$$

Newton's equation and Poisson's law in the quasistatic approximation can be written as

$$\frac{\partial T_{ij}}{\partial x_i}=\rho\frac{\partial v_j}{\partial t}, \tag{12}$$

$$\frac{\partial D_i}{\partial x_i}=0, \tag{13}$$

where $i,j=1,2$, and 3; $v_j=\partial u_j/\partial t$ is the particle velocity; and ρ is the mass density of the medium. Using the generalized vectors and the harmonic time and space dependency, these equations can be reduced to a single matrix relation:

$$\varrho\mathbf{u}=s_1\tau_1+s_2\tau_2+s_3\tau_3, \tag{14}$$

in which matrix ϱ has the form

$$\varrho=\begin{pmatrix} \rho & 0 & 0 & 0 \\ 0 & \rho & 0 & 0 \\ 0 & 0 & \rho & 0 \\ 0 & 0 & 0 & 0 \end{pmatrix}. \tag{15}$$

At this stage, we express τ_1 and τ_3 as functions of τ_2 and $\mathbf{u}$. This is motivated by the fact that the last two vectors are continuous across an interface between two media, so that solutions in two adjacent layers can be related. It is thus possible to introduce the state vector

$$\mathbf{h}=(u_1\ \ u_2\ \ u_3\ \ \phi\ \ \tau_{21}\ \ \tau_{22}\ \ \tau_{23}\ \ \mathcal{D}_2)^T. \tag{16}$$

After some tedious algebra, it is possible to show that $\mathbf{h}$ is a solution inside the nth layer of the eigenvalue problem

$$s_{2,n}\mathbf{h}=M_n\mathbf{h}, \tag{17}$$

in which the 8×8 matrix M_n is given by

$$M_n=\begin{pmatrix} M_{n,11} & M_{n,12} \\ M_{n,21} & M_{n,22} \end{pmatrix}, \tag{18}$$

where

$$M_{n,11}=-A_{22}^{-1}(s_1A_{21}+s_3A_{23}), \tag{19}$$

$$M_{n,12}=A_{22}^{-1}, \tag{20}$$

$$M_{n,21}=-s_1^2(A_{11}-A_{12}A_{22}^{-1}A_{21})-s_3^2(A_{33}-A_{32}A_{22}^{-1}A_{23})$$
$$-s_1s_3(A_{13}+A_{31}-A_{12}A_{22}^{-1}A_{23}-A_{32}A_{22}^{-1}A_{21})$$
$$+\varrho, \quad (21)$$

$$M_{n,22}=-(s_1A_{12}+s_3A_{32})A_{22}^{-1}. \quad (22)$$

The matrix M_n depends on the slownesses s_1 and s_2 and on the material properties. As a consequence, the slownesses $s_{2,n}^{(m)}$ of the eight partial waves can be computed as the eigenvalues of matrix M_n, while the corresponding eigenvectors $F_n^{(m)}$ yield their respective polarizations. Solutions for Eq. (17) can be written in the form

$$\mathbf{h}=F_n\Delta_n(x_2)\mathbf{a}_n, \quad (23)$$

with $\Delta_n(x_2)=\mathrm{diag}[\exp(-\omega s_{2,n}^{(m)}x_2)]$ a diagonal matrix holding the x_2 dependence and $\mathbf{a}_n$ the vector of the amplitudes of the partial waves in the nth layer.

Using the same basic equations, Peach *et al.*[7] arrive at the generalized eigenproblem

$$A_n\mathbf{h}=s_2B_n\mathbf{h}. \quad (24)$$

As in this expression the 8×8 matrix B_n can be inverted, Eq. (24) is equivalent to Eq. (17). The two approaches lead to the same results.

As can be seen from Eq. (10), matrices A_{il} remain well conditioned even if the components of the piezoelectric tensor are zero. For this reason, simple dielectric material can also be treated using this model. In the following, ‘‘piezoelectric’’ will qualify piezoelectric as well as dielectric materials.

B. Case of metal layers

In this work, we assume perfectly conducting metals. Furthermore, we assume that metal layers are grounded, so that the electric potential vanishes on their surfaces. Acoustic propagation inside a metal layer is not coupled to electromagnetic fields. For this reason, the only state equation that can be used for a metal is Hooke's law:

$$T_{ij}=c_{ijkl}S_{kl}, \quad (25)$$

whereas only Newton's law in Eq. (12) is used as the equilibrium equation. Despite these differences, the problem remains the same as for a piezoelectric material except that the electric components must be removed from the generalized stress and displacement vectors. For this reason, and from Eqs. (9) and (14), the dimension of the M_n matrix shrinks from eight to six. Physically speaking, only six purely acoustic partial waves need to be considered.

In addition, the electric displacement is not continuous across an interface between an insulating and a conducting layer. A spatial charge density must then appear at the interface, which equals in modulus the electric displacement at the insulating side of the interface.

C. Case of fluid layers

We are considering perfect fluids that are mechanically isotropic without any viscous effects. Since no electromechanical coupling exists in either conducting or insulating fluids, the mechanical and electrical problems can be treated independently. We first consider conducting fluids, in which no electric components are used, as is the case of metals. We then discuss insulating fluids.

Under the assumptions we have made, the elastic tensor has only one independent component, c,[8] so that

$$c_{ij}=\begin{pmatrix} cI_3 & 0_3 \\ 0_3 & 0_3 \end{pmatrix}. \quad (26)$$

The discussion regarding the calculation of M_n is the same as in the case of a metal layer, with the difference that it can be calculated analytically, since the elastic tensor is the only tensor required and has a very simple expression. It is easy to show that τ_{21} and τ_{23} vanish identically. The state vector then reduces to $\mathbf{h}=(u_1,u_2,u_3,\tau_{22})^T$ and the waves slownesses are found by solving the secular equation

$$|M_n-s_2I_4|=s_2^2\left(s_1^2+s_2^2+s_3^2-\frac{\rho}{c}\right)=0, \quad (27)$$

where ρ is the fluid's mass density.

Equation (27) has a degenerate zero root, that corresponds to two compressive modes in the (x_1,x_3) plane. As they are homogeneous in the thickness of the layer and cannot radiate energy in another layer, we do not consider them in the following. The two other eigenvalues correspond to modes that are either propagating or evanescent in the x_2 direction. Their exact type depends on the characteristic slowness $s_p=\sqrt{\rho/c}$. (i) If $s_1^2+s_3^2<s_p^2$, then the two eigenvalues are real and of opposite sign. The corresponding partial waves are longitudinal and propagating in opposite directions. We will refer to the upward propagating partial wave as ‘‘incident’’ and to the other as ‘‘reflected.’’ (ii) If $s_1^2+s_3^2>s_p^2$, then the partial waves are inhomogeneous. For compatibility, we will use the incident and reflected denominations following the partial wave selection rule given next in Sec. III.

Whatever the eigenvalue, the associated eigenvector always assumes the form

$$u_1=\frac{s_1}{s_2}u_2,$$
$$u_3=\frac{s_3}{s_2}u_2, \quad (28)$$
$$\tau_{22}=\frac{\rho}{s_2}u_2.$$

This shows that only one component of the displacement vector is, indeed, independent. In view of this, we reduce the state vector to $\mathbf{h}=(u_2,\tau_{22})^T$ and the F_n matrix reduces to dimension 2. Table I gives the expressions for the eigenvalues and the F_n matrix for a conducting fluid.

For an insulating fluid, the electrical properties of the layer must be also considered. Therefore, the state vector is expressed as $\mathbf{h}=(u_2,\phi,\tau_{22},\mathcal{D}_2)^T$. The fluid is assumed electrically isotropic so that only one dielectric constant ϵ is needed to describe its electrical properties. In the quasistatic approximation, Poisson's Eq. (13) reduces to the relation

TABLE I. Slownesses and polarization matrices for conducting fluids. s_p is the slowness of the longitudinal mode in the fluid, s_1 and s_3 are the surface slownesses in the x_1 and x_3 directions, ρ is the fluid's mass density, and F is the Fahmy matrix describing the polarizations of partial waves. Also, $s^2=s_1^2+s_3^2$.

	$s^2<s_p^2$: propagating partial waves	$s^2>s_p^2$: inhomogeneous partial waves
Incident partial wave slowness	$s_2=\sqrt{s_p^2-s^2}$	$s_2=j\sqrt{s^2-s_p^2}$
Reflected partial wave slowness	$s_2=-\sqrt{s_p^2-s^2}$	$s_2=-j\sqrt{s^2-s_p^2}$
F matrix	$F=\begin{pmatrix} \lvert s_2\rvert & -\lvert s_2\rvert \\ \rho & \rho \end{pmatrix}$	$F=\begin{pmatrix} j\lvert s_2\rvert & -j\lvert s_2\rvert \\ \rho & \rho \end{pmatrix}$

$$\omega^2\epsilon(s_1^2+s_2^2+s_3^2)\phi=0. \tag{29}$$

Then, we obtain that two electrostatic partial waves exist, with slownesses $s_2=\pm j\sqrt{s_1^2+s_3^2}$, which correspond to evanescent waves. The two electrostatic partial waves are independent of the two acoustic partial waves, which are identical to the two acoustic partial waves for a conducting fluid with the same mass density and independent elastic constant. As in the case of purely acoustic partial waves, we refer to one of them as incident and to the other as reflected. From the Poisson relation we obtain the Fahmy matrix, which is explicitely shown in Table II.

III. SCATTERING MATRIX ALGORITHM

In the previous section, we have shown how to describe fields in a multilayer structure in terms of a superposition of partial waves whose slownesses and polarizations are obtained from the material's constants. The aim of the scattering matrix algorithm is to link the behavior of all layers together in order to obtain the electromechanical response of the whole stratified structure. In the original scattering matrix approach,[4,5] only interfaces between piezoelectric materials were considered. In this work, we consider interfaces between materials of different types, which allows us to study mode conversions at the interfaces.

A. Scattering matrix formulation

It is possible to demonstrate that because of the symmetries of material tensors the eigenvalues of the M_n matrix are found by pairs of conjugate complex or opposite real values.[7] In case the imaginary part of the eigenvalue is not zero, its sign indicates whether the inhomogeneous partial wave is increasing or decreasing with depth inside the layer.

In the scattering method, it is necessary to sort partial waves according to whether they are incident or reflected. The partial wave selection rule used has, for instance, been described in Refs. 4 and 7. Classification is performed using the following rules. (i) Inhomogeneous partial waves are termed reflected if they are evanescent in the medium, whereas they are termed incident if they are growing exponentially with depth. (ii) For propagating waves, power is radiated through the interfaces. The direction in which radiation occurs is given by the sign of the vertical component of the Poynting vector defined by

$$P_2=-\frac{\partial u_i}{\partial t}T_{2,i}+\phi\frac{\partial D_2}{\partial t}=\frac{\omega^2}{2}\mathrm{Re}(\mathbf{u}^{*T}\boldsymbol{\tau}_2). \tag{30}$$

Then, if $P_2>0$, the partial wave is termed reflected, while if $P_2<0$ it is termed incident. In the rest of this article, we will use this rule and add the superscript $(+)$ for incident partial waves and the superscript $(-)$ for reflected ones. Note that the partial mode selection rule has already been applied to fluids in Tables I and II. A graphical representation of the classification rule is shown in Fig. 2.

Once partial waves have been sorted, the F_n, and Δ_n matrices and $\mathbf{a_n}$ vector are reorganized accordingly. Then, Eq. (23) can be rewritten by introducing the auxiliary vector variable $\mathbf{g}_n$ defined by

TABLE II. Slownesses and polarization matrices for insulating fluids. ϵ is the fluid's electric permittivity. Other definitions as in Table I.

	F matrix
Propagating acoustic partial waves	$F=\begin{pmatrix} \sqrt{s_p^2-s^2} & 0 & -\sqrt{s_p^2-s^2} & 0 \\ 0 & 1 & 0 & 1 \\ \rho & 0 & \rho & 0 \\ 0 & j\epsilon s & 0 & -j\epsilon s \end{pmatrix}$
Inhomogeneous acoustic partial waves	$F=\begin{pmatrix} j\sqrt{s^2-s_p^2} & 0 & -j\sqrt{s^2-s_p^2} & 0 \\ 0 & 1 & 0 & 1 \\ \rho & 0 & \rho & 0 \\ 0 & j\epsilon s & 0 & -j\epsilon s \end{pmatrix}$

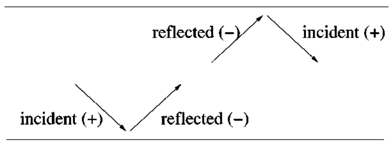

FIG. 2. Representation of incident and reflected waves relative to the bottom surface of a layer.

$$\mathbf{g}_n(x_2)=F_n^{-1}\mathbf{h}(x_2)=\Delta_n(x_2)\mathbf{a}_n =\begin{pmatrix}\Delta_n^{(+)}(x_2) & 0\\ 0 & \Delta_n^{(-)}(x_2)\end{pmatrix}\begin{pmatrix}\mathbf{a}_n^{(+)}\\ \mathbf{a}_n^{(-)}\end{pmatrix}. \quad (31)$$

Here, incident partial waves are stored in the first half of the matrices and vectors, whereas the other half contains the reflected partial waves. With this classification, it is possible to consider independently the restrictions of $\mathbf{g}_n$ to the incident or reflected partial waves, that is, $\mathbf{g}_n^{(+)}=\Delta_n^{(+)}(x_2)\mathbf{a}_n^{(+)}$ and $\mathbf{g}_n^{(-)}=\Delta_n^{(-)}(x_2)\mathbf{a}_n^{(-)}$ respectively.

$\mathbf{g}_n$ can be expressed as a function of $\mathbf{g}_n^{(+)}$ only by introducing a reflexion matrix $R_n(x)$ defined as

$$\mathbf{g}_n^{(-)}(x_2)=R_n(x_2)\mathbf{g}_n^{(+)}(x_2). \quad (32)$$

See Sec. III B for a definition of reflection matrices. Therefore, we have

$$\mathbf{g}_n(x_2)=\begin{pmatrix}I_p\\ R_n(x_2)\end{pmatrix}\mathbf{g}_n^{(+)}(x_2), \quad (33)$$

where $p=1,2,3$, or 4 according to the material type. p is the dimension of the reflection matrix (see Table III). Note that $\mathbf{g}_n(x_2)$ is of dimension $2p$. This shows that the problem can be solved by considering incident waves only.

As can be seen from Eq. (32), the reflection matrix is defined at any position x_2 inside a layer. However, it is only useful to consider R_n^t at the top and R_n^b at the bottom of a given layer in the calculations.

B. Boundary conditions

The first step of the scattering matrix algorithm is to find the reflection matrices at the bottom of the stack. For this, it is possible to assume either a mechanical or an electrical loading. For the sake of simplicity, we only consider here two specific cases, either a semi-infinite substrate or a free bottom surface in a vacuum. The case of a metalized piezoelectric bottom surface can always be treated by adding a vanishingly thin metal layer, which is itself mechanically free.

If the first layer is a semi-infinite substrate, then it can be assumed that no reflection occurs so that

TABLE III. Dimension p of operators and reflexion matrices.

Material type	Dimension of the problem
Piezoelectric	4
Metal	3
Insulating fluid	2
Conducting fluid	1

$$R_1^b=0_p, \quad (34)$$

where 0_p is the square matrix of dimension p whose elements are all zero.

For a plate, the bottom surface is supposed to be stress free and with no electric charge density. This is equivalent to zeroing the lower half of the state vector, whatever the type of layer considered. Then,

$$\mathbf{g}_1(X_0)=F_1^{-1}\begin{pmatrix}I_p\\ 0_p\end{pmatrix}\mathbf{u}=\begin{pmatrix}A\\ B\end{pmatrix}\mathbf{u}, \quad (35)$$

where I_p is the identity matrix of dimension p, A and B are $p\times p$ matrices, and $\mathbf{u}$ is an arbitrary vector. From Eq. (33) it then appears that

$$R_1^b=BA^{-1}. \quad (36)$$

If the first layer is an insulating material the electric behavior of a vacuum under the structure must be taken into account. As was discussed in Sec. II C, a consequence of Poisson's equation in a vacuum is that the relation between normalized electric displacement and electric potential under the structure is

$$\mathcal{D}_2^{(\text{vacuum})}=j\epsilon_0|s|\phi, \quad \text{where} \quad |s|=\sqrt{s_1^2+s_3^2}, \quad (37)$$

so that F_1 in Eq. (35) must be modified according to the rule

$$F_{2p,i}\leftarrow F_{2p,i}-j\epsilon_0|s|F_{p,i} \quad \text{for} \quad i=1\cdots p. \quad (38)$$

It can be noticed that all the content of this subsection is formally similar to what was described in Ref. 4; only the dimension of the matrices involved depends on the type of material considered.

C. Transfer of a reflection matrix

Let us denote x_2 and x_2' two positions inside layer n. From Eqs. (31) and (32) it can be written

$$\mathbf{g}_n^{(-)}(x_2')=\Delta_n^{(-)}(x_2'-x_2)\mathbf{g}_n^{(-)}(x_2) =\Delta_n^{(-)}(x_2'-x_2)R_n(x_2)\Delta_n^{(+)}(x_2-x_2')\mathbf{g}_n^{(+)}(x_2'), \quad (39)$$

that is,

$$R_n(x_2')=\Delta_n^{(-)}(x_2'-x_2)R_n(x_2)\Delta_n^{(+)}(x_2-x_2'). \quad (40)$$

Equation (40) shows how a reflection matrix can be transferred from one point to another within the same layer. It is especially useful for transferring from the bottom to the top of the layer, according to

$$R_n^t=\Delta_n^{(-)}(x_n-x_{n-1})R_n^b\Delta_n^{(+)}(x_{n-1}-x_n). \quad (41)$$

Once again, this derivation is formally similar to what was written in Ref. 4 for piezoelectric layers, but it can be now used for any type of material. As the moduli of all nonzero components of $\Delta_n^{(-)}(x_n-x_{n-1})$ and $\Delta_n^{(+)}(x_{n-1}-x_n)$ involved in Eq. (41) are all smaller than 1, there is no exponential increase of terms of the reflexion matrix. This ensures that the computation of reflexion matrices remains stable whatever the number of layers and their thicknesses.

D. Mode conversions between two layers

We are now considering the interface between layers n and $n+1$. We assume we have been able to calculate R_n^t and we want to determine R_{n+1}^b. By noting $\Delta p = p(n+1) - p(n)$, the difference between the dimensions of the two material types given by Table III, we have to consider three possible cases.

If $\Delta p = 0$, then the interface is between two materials of the same type. It is then possible to write that the state vector is continuous across the interface, so that

$$\mathbf{g}_{n+1}(X_n) = F_{n+1}^{-1} F_n \begin{pmatrix} I_p \\ R_n^t \end{pmatrix} \mathbf{g}_n^{(+)}(X_n) = \begin{pmatrix} A \\ B \end{pmatrix} \mathbf{g}_n^{(+)}(X_n). \quad (42)$$

If $\Delta p > 0$, then the reflection matrix R_{n+1}^b to be determined is of a dimension higher than the known reflection matrix R_n^t. Therefore, the continuity of the state vector cannot be written directly, as the linear system it would lead to would not be well conditioned. To equilibrate the system, additional variables must be introduced, i.e., (i) the electric surface charge density q that can accumulate at the boundary between conducting and insulating layers and (ii) the lateral surface displacements u_1 and u_3 at an interface between fluid and solid layers. Doing so, the relations given in the third column of Table IV, lines 2–5, are obtained. These are of the same type as Eq. (42).

If $\Delta p < 0$, then the reflection matrix R_{n+1}^b to be determined is of a dimension lower than the known reflection matrix R_n^t. Continuity relations cannot be written directly as all components of the state vector in the lower layer are not independent. This is emphasized by the fact that some boundary conditions add supplementary relations to the system, i.e., (i) the electrical potential vanishes at the interface between an insulating and a conductive layer, as it is assumed that all conductive layers are connected to ground, and (ii) the shear stresses τ_{21} and τ_{23} vanish at the interface between a fluid and a solid layer since fluids are supposed ideal. Each of these conditions can be written in the form

$$\sum_{j=1}^{p} M_{kj} \zeta_j = 0, \quad (43)$$

where k is the index of the line affected by the supplementary boundary condition,

$$M = F_n \begin{pmatrix} I_p \\ R_n^t \end{pmatrix}, \quad (44)$$

and where ζ equals $\mathbf{g}_n^{(+)}$ or one of its already reduced forms. It is then possible to express one of the components of ζ, e.g., ζ_{j_0}, as a function of the other components as

$$\zeta_{j_0} = - \sum_{j=1, j \neq j_0}^{p} \frac{M_{k,j}}{M_{i,j_0}} \zeta_j. \quad (45)$$

Defining $\tilde{\zeta}$ as the vector obtained by removing component ζ_{j_0} from ζ, the relation $\zeta = \mathcal{C}\tilde{\zeta}$ holds, where the pivot matrix $\mathcal{C}$ is defined by

$$\mathcal{C}_{i,j} = \delta_{i,j}, 1 \leqslant j < j_0,$$

$$\mathcal{C}_{j_0,j} = - \frac{M_{i,j}}{M_{i,j_0}}, \quad (46)$$

$$\mathcal{C}_{i,j} = \delta_{i,j+1}, j_0 < j \leqslant p.$$

Final expressions for the continuity relation are given in the third column of Table IV, lines 6–10, and are again of the same type as Eq. (42).

In all cases it can be concluded that

$$R_{n+1}^b = B A^{-1}. \quad (47)$$

This reflexion matrix can then be transferred as described in Sec. III C to obtain R_{n+1}^t, which will then be used to compute R_{n+2}^b, and so on, until all reflexion matrices are obtained.

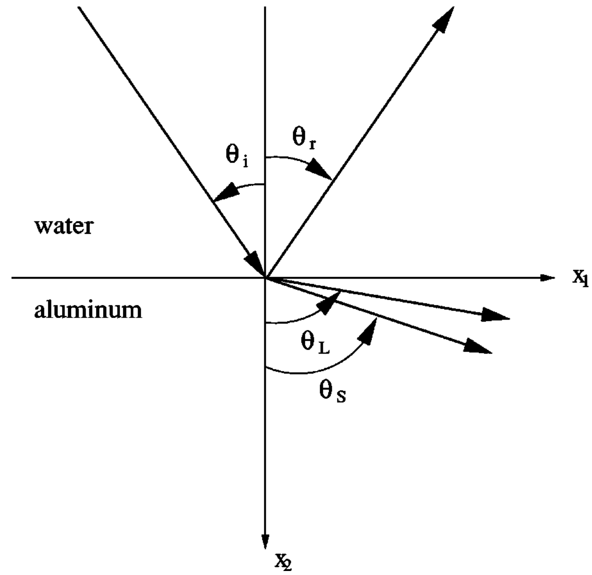

FIG. 3. Conventions for studying the reflection at a fluid/metal interface.

E. Example

As an example of a reflexion matrix calculation let us consider a semi-infinite substrate made of metal (for example aluminum) covered with a half space of water. We focus on the reflexion coefficient of the longitudinal wave in water at the interface between the two media.

As is well known, at small incidence the incident wave splits into a reflected wave propagating back to the liquid medium, and two transmitted waves into the solid, one of a longitudinal polarization and the other of a shear polarization. When the incidence increases and the longitudinal critical angle in aluminum is reached, transmitted longitudinal waves are traveling along the surface and are not transmitted into the solid medium. After the shear critical angle in aluminum there is always total reflection. For a slightly larger angle, there is a sharp phase shift caused by surface waves getting excited at this incidence. All these phenomena can be observed in Fig. 4, which has been calculated assuming $\theta_i = \tan^{-1}(s_1/s_2)$ and with conventions given in Fig. 3. Results in Fig. 4 agree closely with those that can be found in the literature (see e.g., Ref. 9).

TABLE IV. Expressions for calculating the A and B matrices involved in Eq. (47) for each interface type. In these expressions, the projection operator $\mathcal{L}$ restricts a $2p(n)$-component state vector in layer n to its $2p(n+1)$ components that are continuous across the interface with layer $n+1$; $\mathcal{L}$ has dimension $2p(n+1)\times 2p(n)$ and it is assumed that $2p(n+1)<2p(n)$. $\mathcal{L}_N$ is the operator that performs a projection to the u_2 and τ_{22} components only. $\mathcal{C}_\phi$ is the pivot operator that performs the elimination of one unknown through the fact that the electric potential is zero; $\mathcal{C}_{\tau_{21}}$ and $\mathcal{C}_{\tau_{23}}$ are the pivot operators that perform the elimination of one unknown through the fact that the shear stress components must vanish. q is the charge that may have accumulated on electrodes, u_1 and u_3 are the lateral displacements of the solid at the considered interface, and $\tilde{\mathbf{g}}$ is a reduction of the $\mathbf{g}$ vector after pivot operations. P, M, IF, and CF stand, respectively, for piezoelectric, metal, insulating fluid, and conductive fluid.

Interface type	Expression for matrices A and B	Continuity relation
$\Delta p=0$		
P/P, M/M, IF/IF or CF/CF	$\begin{pmatrix}A\\B\end{pmatrix}=F_{n+1}^{-1}F_n\begin{pmatrix}I_p\\R_n^t\end{pmatrix}$	$\mathbf{g}n+1(X_n)=\begin{pmatrix}A\\B\end{pmatrix}\mathbf{g}_n^{(+)}(X_n)$
$\Delta p>0$		
P/M or IF/CF	$\begin{pmatrix}A\\B\end{pmatrix}=F_{n+1}^{-1}\begin{pmatrix}C&0\\0&0\\D&0\\0&1\end{pmatrix}$ where $\begin{pmatrix}C\\D\end{pmatrix}=F_n\begin{pmatrix}I_{p(n)}\\R_n^t\end{pmatrix}$	$\mathbf{g}n+1(X_n)=\begin{pmatrix}A\\B\end{pmatrix}\begin{pmatrix}\mathbf{g}_n^{(+)}(X_n)\\q\end{pmatrix}$
P/IF	$\begin{pmatrix}A\\B\end{pmatrix}=F_{n+1}^{-1}\begin{pmatrix}0&1&0\\c_1&0&0\\0&0&1\\c_2&0&0\\0&0&0\\c_3&0&0\\0&0&0\\c_4&0&0\end{pmatrix}$ where $\begin{pmatrix}c_1\\c_2\\c_3\\c_4\end{pmatrix}=F_n\begin{pmatrix}I_2\\R_n^t\end{pmatrix}$	$\mathbf{g}n+1(X_n)=\begin{pmatrix}A\\B\end{pmatrix}\begin{pmatrix}\mathbf{g}_n^{(+)}(X_n)\\u_1\\u_3\end{pmatrix}$
M/IF or M/CF	$\begin{pmatrix}A\\B\end{pmatrix}=F_{n+1}^{-1}\begin{pmatrix}0&1&0\\c&0&0\\0&0&1\\0&0&0\\d&0&0\\0&0&0\end{pmatrix}$ where $\begin{pmatrix}c\\c'\\d\\d'\end{pmatrix}=F_n\begin{pmatrix}I_3\\R_n^t\end{pmatrix}$ if M/IF or $\begin{pmatrix}c\\d\end{pmatrix}=F_n\begin{pmatrix}1\\R_n^t\end{pmatrix}$ if M/CF	$\mathbf{g}n+1(X_n)=\begin{pmatrix}A\\B\end{pmatrix}\begin{pmatrix}\mathbf{g}_n^{(+)}(X_n)\\u_1\\u_3\end{pmatrix}$
P/CF	$\begin{pmatrix}A\\B\end{pmatrix}=F_{n+1}^{-1}\begin{pmatrix}0&1&0&0\\c&0&0&0\\0&0&1&0\\0&0&0&0\\0&0&0&0\\d&0&0&0\\0&0&0&0\\0&0&0&1\end{pmatrix}$ where $\begin{pmatrix}c\\d\end{pmatrix}=F_n\begin{pmatrix}1\\R_n^t\end{pmatrix}$	$\mathbf{g}n+1(X_n)=\begin{pmatrix}A\\B\end{pmatrix}\begin{pmatrix}\mathbf{g}_n^{(+)}(X_n)\\u_1\\u_3\\q\end{pmatrix}$
$\Delta p<0$		
M/P or CF/IF	$\begin{pmatrix}A\\B\end{pmatrix}=F_{n+1}^{-1}\mathcal{L}F_n\begin{pmatrix}I_{p(n)}\\R_n^t\end{pmatrix}\mathcal{C}_\phi$	$\mathbf{g}n+1(X_n)=\begin{pmatrix}A\\B\end{pmatrix}\widetilde{\mathbf{g}_n^{(+)}(X_n)}$
IF/P or CF/M	$\begin{pmatrix}A\\B\end{pmatrix}=F_{n+1}^{-1}\mathcal{L}F_n\begin{pmatrix}I_{p(n)}\\R_n^t\end{pmatrix}\mathcal{C}_{\tau_{21}}\mathcal{C}_{\tau_{23}}$	$\mathbf{g}n+1(X_n)=\begin{pmatrix}A\\B\end{pmatrix}\widetilde{\mathbf{g}_n^{(+)}(X_n)}$
CF/P	$\begin{pmatrix}a\\b\end{pmatrix}=F_{n+1}^{-1}\mathcal{L}F_n\begin{pmatrix}I_4\\R_n^t\end{pmatrix}\mathcal{C}_\phi\mathcal{C}_{\tau_{21}}\mathcal{C}_{\tau_{23}}$	$\mathbf{g}n+1(X_n)=\begin{pmatrix}a\\b\end{pmatrix}\widetilde{\mathbf{g}_n^{(+)}(X_n)}$
IF/M	$\begin{pmatrix}A\\B\end{pmatrix}=F_{n+1}^{-1}\begin{pmatrix}c&0\\0&0\\d&0\\0&1\end{pmatrix}$ where $\begin{pmatrix}c\\d\end{pmatrix}=\mathcal{L}_NF_n\begin{pmatrix}I_3\\R_n^t\end{pmatrix}\mathcal{C}_{\tau_{21}}\mathcal{C}_{\tau_{23}}$	$\mathbf{g}n+1(X_n)=\begin{pmatrix}A\\B\end{pmatrix}\begin{pmatrix}\widetilde{\mathbf{g}_n^{(+)}(X_n)}\\q\end{pmatrix}$

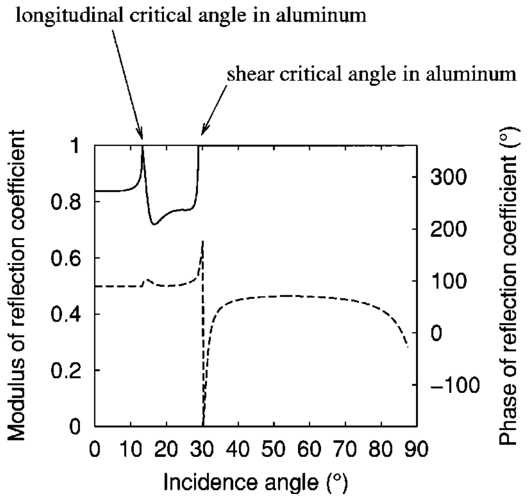

FIG. 4. Reflexion coefficient of a longitudinal wave in water at an interface between water and aluminum.

IV. GREEN'S FUNCTIONS CALCULATION

After the reflexion matrix on top of the multilayer structure has been calculated, the plane wave solution inside the stack of materials is fully determined by the top surface boundary conditions. More generally, it becomes possible to link the generalized displacements, that is, the first part of the state vector, to the generalized strain, which is its second part, and thus to obtain the Green's functions of the multilayer. Writing Eq. (33) on top of the last layer yields

$$\mathbf{h}(X_N)=F_N\mathbf{g}_N(X_N)=F_N\begin{pmatrix} I_p \\ R_N^t \end{pmatrix}\mathbf{g}_N^{(+)}(X_N)=\begin{pmatrix} E \\ F \end{pmatrix}\mathbf{g}_N^{(+)}(X_N), \tag{48}$$

from which we get the expression for the Green's function matrix or dyadic as

$$G=EF^{-1}, \tag{49}$$

where E and F are square matrices of dimension $p(N)$.

In particular, if the topmost layer is piezoelectric, once the Green's functions are known, it is possible to obtain a relation between the electric charge density that appears under the electrode in absence of mechanical loading and the electrode potential, and thus the electric response of a structure as

$$Y=\omega^2 G_{44}^{-1}. \tag{50}$$

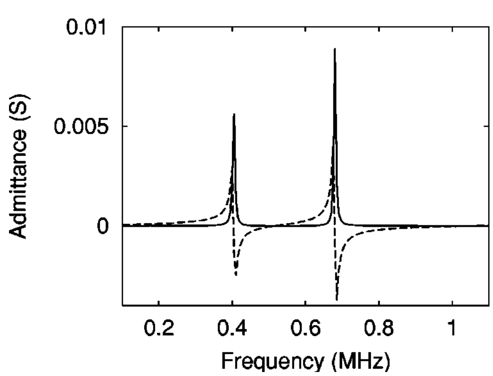

FIG. 5. Electrical response of an ultrasound transducer with its adaption layer.

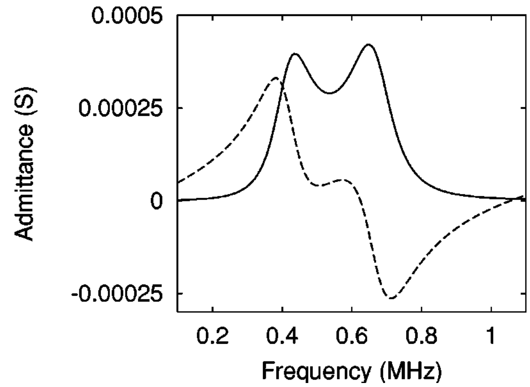

FIG. 6. Electrical response of an ultrasound transducer radiating in water.

The ω^2 term must be included since we have chosen to use $\mathcal{D}_2=D_2/(j\omega)$ in the state vector.

In the same way, it becomes possible to calculate the effective permittivity,[10] which is also simply related to G_{44} through

$$\epsilon_{\mathrm{eff}}=\frac{\omega}{\epsilon_0|s_1|G_{44}}. \tag{51}$$

As an example let us consider an ultrasound transducer consisting of a 2-mm-thick PZT layer covered by a quarter-wavelength layer. We assume excitation electrodes are infinitely thin so that their mechanical effect is negligible. Figure 5 shows the electric response of such a structure. It agrees with similar responses that have been obtained by finite-element analysis or using Mason's model.[11] In Fig. 6 a semi-infinite medium of water has been added. Radiation losses cause the two peaks to degenerate into a wide-band response, which is usually what is wanted when designing ultrasound transducers.

V. BACKSCATTERING THROUGH THE STACK

As already stated, the behavior of waves in the structure is known once all reflexion matrices have been calculated. Making use of this property effectively, the amplitudes of all partial waves can be calculated so that all electromechanical fields can be determined through Eq. (23). In this section, we assume the structure is electrically excited at its top surface, and that the topmost layer is piezoelectric. The electric permittivity of the surrounding vacuum is taken into account as described in Sec. III B, Eq. (38).

Boundary conditions at the top surface can be written in the form

$$LF_n\begin{pmatrix} I_4 \\ R_N^t \end{pmatrix}\mathbf{g}_N^{t(+)}=M\mathbf{g}_N^{t(+)}=\begin{pmatrix} 1 \\ 0 \\ 0 \\ 0 \end{pmatrix}, \tag{52}$$

where

$$L=\begin{pmatrix} 0 & 0 & 0 & 1 & 0 & 0 & 0 & 0 \\ 0 & 0 & 0 & 0 & 1 & 0 & 0 & 0 \\ 0 & 0 & 0 & 0 & 0 & 1 & 0 & 0 \\ 0 & 0 & 0 & 0 & 0 & 0 & 1 & 0 \end{pmatrix}, \tag{53}$$

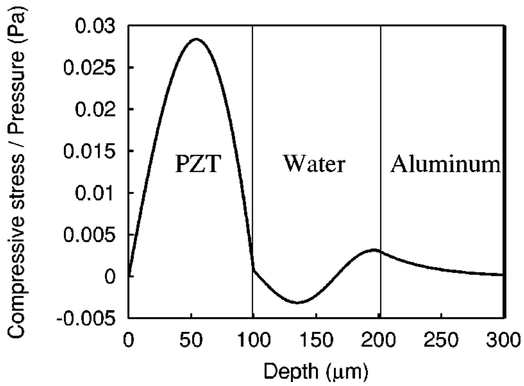

FIG. 7. Standing wave pattern for a wave excited by a piezoelectric transducer in water incident on an aluminum substrate with Rayleigh incidence.

and, in this case,

$$\mathbf{a}_N = \Delta_N^{(+)}(-X_N)M^{-1}\begin{pmatrix}1\\0\\0\\0\end{pmatrix}. \tag{54}$$

Reflected modes are known from the reflection matrix on top of the layer. Amplitudes of partial modes in the other layers are then computed using a recursive scheme. We have shown in Sec. III C that for every interface between two layers it is possible to write

$$\mathbf{g}_{n+1}(X_n) = \begin{pmatrix}A\\B\end{pmatrix}\widetilde{\mathbf{g}_n}^{(+)}(X_n), \tag{55}$$

where expressions for A, B, and $\widetilde{\mathbf{g}_n}^{(+)}(X_n)$ are given in Table IV. Therefore,

$$\widetilde{\mathbf{a}_n}^{(+)} = \Delta_n^{(+)}(-X_n)A^{-1}\mathbf{g}_{n+1}^{(+)}(X_n). \tag{56}$$

The actual $\mathbf{a}_n^{(+)}$ vector is obtained (i) directly if $\Delta p = 0$, (ii) by keeping only the first relevant components if $\Delta p > 0$, and (iii) by expressing the components that have been removed as a function of the ones that have been kept if $\Delta p < 0$.

Amplitudes of partial reflected modes are calculated using the reflexion matrix at the top of the layer and the amplitudes of partial transmitted modes, as shown in Eq. (32). As the A matrices have already been calculated in the reflection matrices computation step, backscattering becomes very fast to perform.

A. Example

Let us go back to the example started in Sec. III E. We assume that waves are excited by a simple piezoelectric transducer radiating in water and that the incident wave reaches the water/aluminum interface close to the Rayleigh incidence. To simulate this situation, s_1 is set so that $\theta_i = \tan^{-1}(s_1/s_p) \approx 30°$. In Fig. 7, T_{22} in solids and the acoustic pressure in water are plotted versus the depth inside the structure. The transducer operates in a half-wavelength mode and radiates in water. The stress vanishes smoothly with depth inside the aluminum as the incidence is above the shear critical angle. A standing wave pattern is established inside the two first layers because of the total reflection at the upper interface and on the aluminum half space.

VI. CONCLUSION

We have shown how to introduce metal and fluid layers into a scattering matrix model originally proposed for solving the problem of plane wave propagation in piezoelectric and dielectric multilayers. This scattering matrix approach is naturally numerically stable as opposed to transfer matrix approaches. The incorporation of fluid and metal layers was made possible by reducing the number of plane waves that can propagate inside a layer and the dimension of the linear system that has to be solved for each layer. We have also shown that despite the possible difference in dimensions between two layers, it is possible to add or remove an adequate number of unknowns when writing that some electromechanical fields are continuous or not across the interface. Therefore, it becomes possible to compute the surface Green's functions of an arbitrary stack of homogeneous materials with plane interfaces. Additionally, we have set up a backscattering algorithm to compute the distribution of partial modes inside the whole layered structure. This latter approach is particularly important to understand the distribution of acoustoelectric power within the stacked substrate. In many ultrasonic works, much effort is made to correctly simulate actual boundary conditions, but generally the wave distribution is not regarded. It is, however, of primary importance to precisely analyze this distribution in layered materials in view of optimizing the transducer structure. As it is possible to derive Green's functions that can be coupled to more complete models (e.g., finite element method/boundary element method),[12] our approach provides an attractive way to enrich the analysis capabilities of elastic waveguides and, more generally, of electromechanical transducers.

ACKNOWLEDGMENTS

The authors wish to thank J. Desbois, Y. Fusero, and M. Wilm for fruitful discussions. T. Lemoine from Thales Research and Technology, France, and W. Steichen and M. Solal from Temex Microsonics are gracefully acknowledged for support in this work.

[1] A. H. Fahmy and E. L. Adler, Appl. Phys. Lett. **22**, 495 (1973).
[2] E. L. Adler, IEEE Trans. Ultrason. Ferroelectr. Freq. Control **37**, 485 (1990).
[3] M. J. S. Lowe, IEEE Trans. Ultrason. Ferroelectr. Freq. Control **42**, 525 (1995).
[4] T. Pastureaud, V. Laude, and S. Ballandras, Appl. Phys. Lett. **80**, 2544 (2002).
[5] E. L. Tan, IEEE Trans. Ultrason. Ferroelectr. Freq. Control **49**, 929 (2002).
[6] ANSI/IEEE Standard No. 176-1987 (1987).
[7] R. Peach, IEEE Trans. Ultrason. Ferroelectr. Freq. Control **48**, 1308 (2001).
[8] D. Royer and E. Dieulesaint, *Elastic Waves in Solids* (Springer, New York, 2000), Vol. 1.
[9] J. D. N. Cheeke, *Fundamental and Applications of Ultrasonic Waves* (CRC, Boca Raton, FL, 2002), Chap. 7, pp. 128–138.
[10] K. A. Ingebrigtsen, J. Appl. Phys. **40**, 2681 (1969).
[11] G. S. Kino, *Acoustic Waves, Devices, Imaging and Analog Signal Processing* (Prentice-Hall, Englewood Cliffs, NJ, 1987).
[12] P. Ventura, J. M. Hodé, J. Desbois, and M. Solal, IEEE Trans. Ultrason. Ferroelectr. Freq. Control **48**, 1259 (2001).